Experimental Evidence of a Variant Neutron Spectrum from the $T(t,2n)\alpha$ Reaction at Center-of-Mass Energies in the Range of 16–50 keV

M. Gatu Johnson,[1,*] C. J. Forrest,[2] D. B. Sayre,[3] A. Bacher,[4] J.-L. Bourgade,[5] C. R. Brune,[6] J. A. Caggiano,[3] D. T. Casey,[3] J. A. Frenje,[1] V. Yu. Glebov,[2] G. M. Hale,[7] R. Hatarik,[3] H. W. Herrmann,[7] R. Janezic,[2] Y. H. Kim,[7] J. P. Knauer,[2] O. Landoas,[5] D. P. McNabb,[3] M. W. Paris,[7] R. D. Petrasso,[1] J. E. Pino,[3] S. Quaglioni,[3] B. Rosse,[5] J. Sanchez,[3] T. C. Sangster,[2] H. Sio,[1] W. Shmayda,[2] C. Stoeckl,[2] I. Thompson,[3] and A. B. Zylstra[7]

[1]*Massachusetts Institute of Technology Plasma Science and Fusion Center, Cambridge, Massachusetts 02139, USA*
[2]*Laboratory for Laser Energetics, University of Rochester, Rochester, New York 14623, USA*
[3]*Lawrence Livermore National Laboratory, Livermore, California 94550, USA*
[4]*Indiana University, Bloomington, Indiana 47405, USA*
[5]*CEA, DAM, DIF, F-91297 Arpajon, France*
[6]*Ohio University, Athens, Ohio 45701, USA*
[7]*Los Alamos National Laboratory, Los Alamos, New Mexico 87544, USA*

(Received 2 August 2017; revised manuscript received 20 March 2018; published 27 July 2018)

Full calculations of six-nucleon reactions with a three-body final state have been elusive and a long-standing issue. We present neutron spectra from the $T(t,2n)\alpha$ (TT) reaction measured in inertial confinement fusion experiments at the OMEGA laser facility at ion temperatures from 4 to 18 keV, corresponding to center-of-mass energies ($E_{\mathrm{c.m.}}$) from 16 to 50 keV. A clear difference in the shape of the TT-neutron spectrum is observed between the two $E_{\mathrm{c.m.}}$, with the ^{5}He ground state resonant peak at 8.6 MeV being significantly stronger at the higher than at the lower energy. The data provide the first conclusive evidence of a variant TT-neutron spectrum in this $E_{\mathrm{c.m.}}$ range. In contrast to earlier available data, this indicates a reaction mechanism that must involve resonances and/or higher angular momenta than $L = 0$. This finding provides an important experimental constraint on theoretical efforts that explore this and complementary six-nucleon systems, such as the solar $^3\mathrm{He}(^3\mathrm{He},2p)\alpha$ reaction.

DOI: 10.1103/PhysRevLett.121.042501

The six-nucleon reaction between two tritons $T(t,2n)\alpha$ (TT) has proven challenging to determine theoretically, because it produces three particles in the final state [1–4]. Accurate experimental data are required to guide the theoretical efforts. Available cross section data for this reaction [5–10], although relatively inaccurate, are consistent with a flat S factor below center-of-mass energy $E_{\mathrm{c.m.}} = 500$ keV. Measurements by Wong, Anderson, and McClure [11] as a function of the angle also indicate an isotropic cross section at $E_{\mathrm{c.m.}} = 160$ keV. Combined, these two observations suggest that an s-wave reaction channel ($L = 0$) dominates in this $E_{\mathrm{c.m.}}$ range and that any resonance contributions arise from very broad states. This interpretation, which is also consistent with theoretical studies using a microscopic model [12] and R-matrix methods [13], would mean that the shape of the reaction product energy spectra would be independent of $E_{\mathrm{c.m.}}$. In contrast, Casey *et al.* [14] explored the idea based on the limited previous TT-neutron spectral data [11,14–18] that the shape may possibly depend on $E_{\mathrm{c.m.}}$. However, due to widely varying systematics between the different measurements in combination with large uncertainties, such a dependence has not been demonstrated.

In this Letter, we report on accurate new measurements of the TT reaction at $E_{\mathrm{c.m.}}$ in the range 16–50 keV at the OMEGA laser [19], which provide the first conclusive demonstration of an $E_{\mathrm{c.m.}}$ dependence in the TT-neutron spectrum. This result indicates a reaction mechanism that, unexpectedly, must involve resonances and/or higher angular momenta than $L = 0$. These findings may also have implications for the $^3\mathrm{He}(^3\mathrm{He},2p)\alpha$ ($^3\mathrm{He}^3\mathrm{He}$) mirror reaction, which plays an important role in the solar proton-proton (pp) chains [20]. The S factor for this reaction is inferred based on accelerator measurements of the $^3\mathrm{He}^3\mathrm{He}$ reaction rate [20–24]. In particular, measurements at solar-fusion-relevant energies were obtained at the LUNA underground accelerator facility [20,22–23], where the setup allows for measurement of $^3\mathrm{He}^3\mathrm{He}$ protons with energies above 2.75 MeV. The analysis and interpretation of the LUNA data rely on an extrapolation to energies below 2.75 MeV assuming an elliptical proton spectrum for a determination of the total $^3\mathrm{He}^3\mathrm{He}$ reaction rate [23]. As our findings suggest that the $^3\mathrm{He}^3\mathrm{He}$ proton spectral shape likely varies with $E_{\mathrm{c.m.}}$, the use of an elliptical spectrum in the analysis of the LUNA $^3\mathrm{He}^3\mathrm{He}$ data may not be adequate. As an example, if the R-matrix spectral shape

TABLE I. Summary of parameters for the three OMEGA implosions studied in this paper. The $E_{\mathrm{c.m.}}$ values quoted represent the peak values for the $E_{\mathrm{c.m.}}$ distributions shown in Fig. 1.

Shot	Pulse shape	Laser energy (kJ)	Capsule diameter (μm)	Shell thickness (μm)	T_2 fill pressure (atm)	TT-n yield ($\times 10^{12}$)	DT T_{ion} (keV)	$E_{\mathrm{c.m.}}$ (keV)
77951	0.6 ns square	16.1	1004	2.9	3.3	0.49 ± 0.05	18.3 ± 0.5	50
77960	0.6 ns square	16.1	1004	2.9	8.2	1.27 ± 0.14	11.1 ± 0.5	36
77963	2 ns ramp	24.1	1009	3.0	8.2	0.24 ± 0.03	3.7 ± 0.5	16

calculated by Brune *et al.* [25] was used instead for this extrapolation, the inferred ^{3}He^{3}He reaction rate would be 8% higher than reported. With a total estimated uncertainty of 4% for the ^{3}He^{3}He S factor [20], such an adjustment would have an impact on the ppI/(ppII + ppII) branching ratio and hence on solar neutrino physics, motivating the need for a deeper understanding of the shape of the ^{3}He^{3}He proton spectrum.

The experiment reported herein was explicitly designed to generate a range of ion temperatures (T_{ion}) (hence $E_{\mathrm{c.m.}}$) to accurately study the TT-neutron spectrum at different $E_{\mathrm{c.m.}}$ while maintaining identical measurement conditions. Glass capsules (1 mm outer diameter, 3 μm shell thickness) were filled with 3.2 or 8.2 atm of T_2 gas with 0.36% and 0.15% deuterium impurity by atom, respectively, and irradiated with the 60 OMEGA laser beams directly incident on the capsule. T_{ion} (inferred from the broadening of measured DT neutron spectra [26]) was tuned by varying the laser pulse shape and beam focus together with the gas-fill pressure [27]. A neutron-averaged $T_{\mathrm{ion}} = 18.3 \pm 0.5$ keV was obtained by irradiating a low-pressure target with a square pulse with 0.6 ns duration delivering 16 kJ of energy with the laser beams focused to the center of the capsule. A 2.0-ns ramped laser pulse delivering 24 kJ energy onto the high-pressure capsule with defocused beams provided a T_{ion} of 3.7 ± 0.5 keV. An intermediate-temperature case was obtained by imploding a high-pressure capsule with the 0.6 ns square pulse delivering 16 kJ of energy with all the beams focused to the center of the capsule ($T_{\mathrm{ion}} = 11.1 \pm 0.5$ keV). The duration of burn was about 0.2 ns for all implosions. Resulting implosion parameters are summarized in Table I. Calculated burn-averaged $E_{\mathrm{c.m.}}$ distributions for the three implosions are shown in Fig. 1. The reactions occur over a range of $E_{\mathrm{c.m.}}$ because of the thermal ion-velocity distributions in these inertial confinement fusion (ICF) experiments [28]. Additionally, T_{ion} is not uniform throughout an ICF implosion; this was considered in the calculation of the distributions in Fig. 1 by using radial temperature and density profiles from 1D radiation-hydrodynamics simulations with the code HYADES [29], constrained to match measured T_{ion} (see Ref. [27] for details). These calculations also show that the DT and TT burn-averaged T_{ion} are expected to be virtually the same for these implosions. Average $E_{\mathrm{c.m.}}$ of 16, 36, and 50 keV are inferred for the implosions with $T_{\mathrm{ion}} = 3.7$, 11.1, and 18.3 keV, respectively.

The TT-neutron spectra generated in this experiment were measured with a neutron time-of-flight (NTOF) spectrometer located 13.4 m from the implosion with a well-collimated line of sight [30–32] (see Ref. [30], Fig. 4, for a sketch of the setup). This spectrometer consists of an 8×4"(diameter x thickness) oxygenated xylene scintillator coupled to four photomultiplier tubes (PMTs) with different sensitivities. Two of the PMTs, a Photek [33] model 140 (PMT-A) and a Photek model 240 (PMT-D), were set up to measure the TT-neutron spectrum. Output signals were recorded using fast (1 GHz) oscilloscopes. The impulse response of the spectrometer was measured *in situ* using a 10-ps-wide x-ray impulse, independently for PMT-A and PMT-D. The neutron response was subsequently obtained by folding the x-ray impulse with energy-dependent beam line neutron attenuation, neutron transport time through the detector, and scintillator light output. The detector sensitivity drops gradually with decreasing neutron energy due to a larger time spread and less light generated in the scintillator material. Two different xylene light-yield-versus-energy curves, published by Verbinski *et al.* [34] and Craun and Smith [35], were used in the analysis presented here. The choice of light-yield curve or PMT does not impact the conclusion that the TT-neutron spectrum changes with varying $E_{\mathrm{c.m.}}$; rather, these choices lead to uncertainties in the spectral decomposition, which is quantified in Fig. 4.

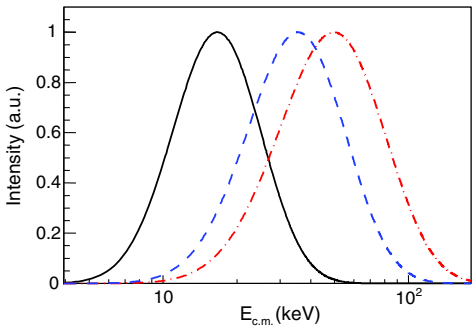

FIG. 1. Calculated center-of-mass energy distributions for the implosions with $T_{\mathrm{ion}} = 3.7$ keV (solid black curve), $T_{\mathrm{ion}} = 11.1$ keV (dashed blue curve), and $T_{\mathrm{ion}} = 18.3$ keV (dash-dotted red curve).

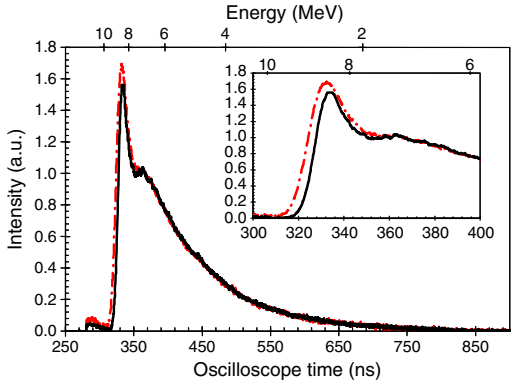

FIG. 2. NTOF-measured signal traces for shots 77951 (dash-dotted red curve, $T_{\rm ion} = 18.3$ keV) and 77963 (solid black curve, $T_{\rm ion} = 3.7$ keV). The time axis has been corrected for capsule burn time (0.8 ns for 77951 and 1.7 ns for 77963). The corresponding neutron energy scale is indicated at the top. The traces are normalized to match in the time interval 361–371 ns (6.8–7.2 MeV neutron energy). The inset shows an enlargement of the ^{5}He gs peak at $E_n = 8.6$ MeV.

The measured NTOF signal traces for shots 77951 and 77963 are shown in Fig. 2. Both traces show a small residual DT signal tail at 280 ns, immediately prior to the TT signal rise at 320 ns; this residual DT level is used to constrain the DT background in the fits (see Fig. 3). (As the DT-neutron peak at 14 MeV is gated out in the measurement, the sharp rise at 280 ns represents the turn-on of the gate.) The DT background is slightly higher relative to the TT signal for shot 77951 than for shot 77963 due to a higher D-impurity level in the low-pressure fill versus the high-pressure fill (0.36% versus 0.15%, respectively). However, in both cases the D-impurity level is small enough that the impact of the DT-neutron background on the measurement of the TT-neutron spectrum is negligible. A peak associated with the ^{5}He ground state (gs) n-α interaction (at $E_n = 8.6$ MeV) is clearly observed in both time-of-flight spectra. This peak as well as the entire spectrum are broadened both by the NTOF instrument response and thermal Doppler broadening proportional to the square root of $T_{\rm ion}$ of the reacting ions [26]. The thermal broadening is different for shot 77951 (0.53 MeV FWHM) than for shot 77963 (0.24 MeV FWHM), which has to be considered in the comparison of the spectra. However, keeping this in mind, inspection of the raw signal traces in Fig. 2 clearly shows that the ^{5}He gs peak is stronger relative to the continuum for the high-temperature implosion, 77951, than for the low-temperature implosion, 77963. Quantitatively, the ratio of signal in the 314–350 ns range to the 366–484 ns range (roughly corresponding to neutron energies 7.7–9.5 and 4–7 MeV) is 0.57 for shot 77951 and 0.45 for shot 77963. The ratio for shot 77960 with intermediate $E_{\rm c.m.} = 36$ keV (not shown in Fig. 2) falls between the two at 0.50, indicating a gradual change in the spectrum with varying $E_{\rm c.m.}$.

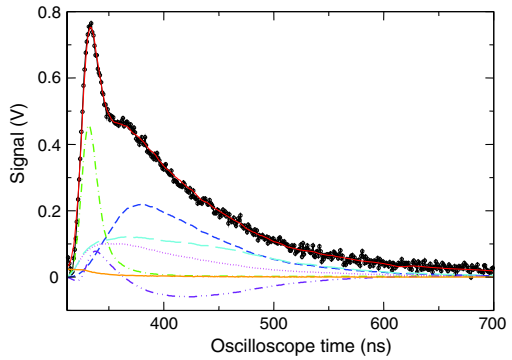

FIG. 3. Total R-matrix fit (solid red curve) to measured NTOF data for shot 77951 (black points) with $T_{\rm ion} = 18.3$ keV using the Verbinski light-yield function. Also shown in the figure are the R-matrix components representing the $3/2^-$ (dash-dotted green curve), $1/2^-$ (short-dashed blue curve), and $1/2^+$ (dotted magenta curve) partial waves and the dineutron (nn) interaction (long-dashed cyan curve), an interference component (double-dot-dashed purple curve), and the contribution from the DT neutron background (solid orange curve). The DT background level is constrained by the small DT tail visible before the rise of the TT spectrum (compare Fig. 2).

To enable quantitative comparison of the measured TT-neutron spectra at the different c.m. energies, the PMT-A and PMT-D- measured NTOF signals are analyzed using a forward-fit approach (using both Verbinski and Craun and Smith light-yield curves) with the phenomenological R-matrix model described in Ref. [25], with six feeding factors as free parameters. Thermal Doppler broadening of the spectra is considered in the analysis. As the statistical uncertainty in the measured spectra is dominated by oscilloscope digitization noise, it is challenging to assign realistic error bars to the 402 individual data points. This was handled in the analysis by assigning data-point errors that give reduced $\chi^2 = 1$ for a 3rd degree polynomial fit to a slow-varying region of the spectrum (370–520 ns). As an example, the resulting R-matrix fit to the PMT-A spectrum for shot 77951 using the Verbinski light-yield curve is shown in Fig. 3. With statistical error bars as described above, a $\chi^2_{\rm red} = 2.0$ is determined for this fit [36]. Also shown in Fig. 3 are the individual R-matrix components comprising the fit, including a component to account for net interference between all partial waves (see Ref. [25] for details).

The R-matrix feeding factors resulting from the fits to the PMT-D spectra using the Craun and Smith light-yield curve are summarized in Table II, together with the statistical uncertainty in each case (a full summary of all inferred feeding factors and $\chi^2_{\rm red}$ from each fit can be found in Supplemental Material [37]). The underlying assumption of the R-matrix analysis is that the TT reaction proceeds through the s wave ($L = 0$, $J = 0^+$) only. Two levels (λ in Table II) are considered for each partial wave in the $\alpha + n$

TABLE II. Feeding factors inferred from R-matrix fits to shots 77951 ($T_{\rm ion} = 18.3$ keV, $E_{\rm c.m.} = 50$ keV), 77060 ($T_{\rm ion} = 11.1$ keV, $E_{\rm c.m.} = 36$ keV), and 77963 ($T_{\rm ion} = 3.7$ keV, $E_{\rm c.m.} = 16$ keV).

		$A_{c\lambda}$		
Ch	λ	77951	77960	77963
$1/2^+$	1	$-24.4 \pm 1.1_{\rm stat}$	$-27.7 \pm 1.6_{\rm stat}$	$-18.6 \pm 1.6_{\rm stat}$
$1/2^+$	2	0	0	0
$1/2^-$	1	$-16.8 \pm 0.1_{\rm stat}$	$-17.5 \pm 0.2_{\rm stat}$	$-18.2 \pm 0.1_{\rm stat}$
$1/2^-$	2	$-218 \pm 5_{\rm stat}$	$-128 \pm 8_{\rm stat}$	$-292 \pm 7_{\rm stat}$
$3/2^-$	1	$9.81 \pm 0.03_{\rm stat}$	$9.08 \pm 0.04_{\rm stat}$	$8.85 \pm 0.03_{\rm stat}$
$3/2^-$	2	$223 \pm 3_{\rm stat}$	$242 \pm 4.1_{\rm stat}$	$240 \pm 3_{\rm stat}$
nn	1	$13.8 \pm 0.2_{\rm stat}$	$15.1 \pm 0.2_{\rm stat}$	$14.7 \pm 0.2_{\rm stat}$

system, and one partial wave or level is assumed for the dineutron system (nn). Each level has a feeding factor $A_{c\lambda}$, determined by the fit to the data, and its sign determines the interferences between individual waves and channels. The $3/2^-$ partial wave describes the peak seen at 340 ns ($E_n = 8.6$ MeV), which can be distinguished well from the broad continuum that follows. The feeding factor for the $3/2^-$, $\lambda = 1$ state increases in strength over the investigated $E_{\rm c.m.}$, in unison with the high-energy peak in the spectrum. (The $3/2^-$, $\lambda = 2$ state, which also contributes to the $3/2^-$ component in Fig. 3, lies mainly in the continuum).

The fully reduced TT-neutron spectra for shots 77951 and 77963, with NTOF instrument response and thermal Doppler broadening removed, are contrasted in Fig. 4. These final spectra represent the average of the spectra obtained using the Craun and Smith and Verbinski light-yield curves and PMT-A and PMT-D data in the analysis. The linewidth represents the total systematic uncertainty defined as the difference between the average and each extreme. The ^{5}He gs peak is clearly more pronounced for the spectrum measured at $E_{\rm c.m.} = 50$ keV than for the

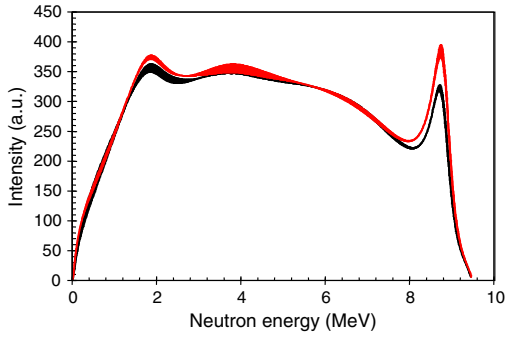

FIG. 4. Final neutron spectra inferred from R-matrix analysis of the measured NTOF-spectra for shot 77951 (red curve, $E_{\rm c.m.} = 50$ keV) and 77963 (black curve, $E_{\rm c.m.} = 16$ keV), normalized to each other in the 4–7 MeV range. The width of the lines represents the estimated systematic uncertainty. These spectra clearly demonstrate a difference in the shape of the neutron spectrum with the peak at 8.6 MeV corresponding to the ^{5}He gs interaction being stronger at a higher energy.

$E_{\rm c.m.} = 16$ keV case. Note that the peak at 2 MeV is also associated with the ^{5}He gs; this enhancement in the spectrum corresponds to the subsequent decay of ^{5}He into a neutron and an alpha particle.

The underlying physics behind the observed $E_{\rm c.m.}$ dependence is not clear. As stated in the introduction, previous data for this reaction are consistent with only s waves involving very broad states, in which case the spectral shape would be independent of energy. The observed $E_{\rm c.m.}$ dependence indicates a more complicated reaction mechanism that must involve resonances and/or higher angular momenta than $L = 0$. Theoretical calculations by Thomson and Tang using a resonating group model [38] and more recently by Arai, Kato, and Aoyama using a microscopic cluster model [39] suggest the presence of a 0^- resonance of ^{6}He around 0.5 MeV above the TT threshold and with a large width (~4 MeV). *Ab initio* calculations of the $^4{\rm He} + n + n$ continuum carried out using a soft NN interaction that accurately describes nucleon-nucleon data also suggest the presence of 0^- resonances near the TT threshold [4]. The present experiment may be probing the low-energy tail of this resonance and the way it decays. If this is the case, the observed spectra will have s-wave and p-wave channel contributions, and it is not unreasonable to think that the p-wave contributions may increase with higher $E_{\rm c.m.}$, as we approach the 0^- resonance. The possible ways of forming an $n + {}^5{\rm He}$ 0^- state are (i) $n(1/2^+) + {}^5{\rm He}(1/2^+)$, with $S = 1$, $L = 1$, (ii) $n(1/2^+) + {}^5{\rm He}(1/2^-)$, with $S = 0$, $L = 0$, and (iii) $n(1/2^+) + {}^5{\rm He}(3/2^-)$, with $S = 2$, $L = 2$.

The first two channels are Pauli suppressed, because the s shell is complete. Hence, channel (iii) will be dominant. This channel requires a relative angular momentum $L = 2$ between the neutron and the ^{5}He. Given the large Q value of the TT reaction, there is most likely enough energy in the system to allow $L = 2$ for $^5{\rm He} + n$. As we have seen, the ^{5}He $3/2^-$ state gives rise to the peak at the high-energy edge of the TT-neutron spectrum. This suggests that if the p-wave contribution increases with energy, then the relative intensity of the ^{5}He $3/2^-$ peak is also expected to increase, as observed.

An alternative explanation is that there could be a 0^+, $T = 1$ excited state in ^{6}He above the ground state, in the vicinity of the TT-reaction threshold, with a total width sufficiently narrow to cause the observed change in spectral shape over 30 keV in excitation energy. It is notoriously hard to detect a 0^+ resonance in scattering, because most s-wave phase shifts look like hard-sphere phases, and the presence of a resonance modifies that behavior only slightly. A fit to the limited sets of data that exist for ^{6}He [TT differential elastic scattering cross sections and $T(t, 2n)\alpha$ cross sections] gives (in addition to the ground-state level) a broad 0^+ resonance at an excitation energy of 13.65 MeV and a negative parity resonance at 14.38 MeV.

The data set reported herein demonstrates an energy dependence in the TT-neutron spectral shape in the range of $E_{\mathrm{c.m.}} = 16$–50 keV but does not conclusively distinguish between different theoretical hypotheses for explaining this observation. This means that it is impossible to predict how the spectral shape will evolve with further varying $E_{\mathrm{c.m.}}$ on the basis of currently available information. Such predictions would require full *ab initio* calculations including all possible resonances, which are not currently available. If, e.g., 0^- is responsible for the observed $3/2^-$ peak enhancement with $E_{\mathrm{c.m.}}$, then we may expect this peak to remain low towards lower energy and increase in importance towards higher energy until the energy is above the resonance, at which point it may again start to decrease (unless other resonances come into play at this higher energy). Note also that if the energy dependence observed in the TT-neutron spectrum is due to 0^- or 0^+ resonances as suggested here, then equivalent energy dependencies are expected also for the ^{3}He^{3}He reaction, although shifted in energy due to the Coulomb barrier. This observation should motivate further theoretical investigations of the few-body physics governing these six-nucleon systems and provide guidance for ongoing *ab initio* efforts [2–4].

In conclusion, using the OMEGA laser to implode T_2-gas-filled thin-glass-shell capsules, the TT-neutron spectrum has been studied at $E_{\mathrm{c.m.}}$ of 16, 36, and 50 keV. For the first time, the resulting data conclusively demonstrate an energy dependence in the spectral shape over this $E_{\mathrm{c.m.}}$ range. This observation indicates a more complicated reaction mechanism than the s-wave only previously assumed for this reaction. In particular, the relative strength of the peak associated with the $3/2^-$ ^{5}He ground state is found to increase with increasing $E_{\mathrm{c.m.}}$, possibly indicating the impact of a 0^- p-wave resonance. An equivalent energy dependence for the mirror ^{3}He^{3}He reaction could impact analysis of accelerator measurements used as the basis for evaluation of the ^{3}He^{3}He S factor at solar-fusion energies.

This material is based upon work supported by the Department of Energy, National Nuclear Security Administration under Awards No. DE-NA0001857, No. DE-NA0002949, and No. DE-NA0002905, and Office of Science under Award No. DE-FG02-88ER40387. The work was also supported in part by National Laser Users' Facility (DE-NA0002035) and LLE (415935-G). This report was prepared as an account of work sponsored by an agency of the U.S. Government. Neither the U.S. Government nor any agency thereof, nor any of their employees, makes any warranty, express or implied, or assumes any legal liability or responsibility for the accuracy, completeness, or usefulness of any information, apparatus, product, or process disclosed, or represents that its use would not infringe privately owned rights. Reference herein to any specific commercial product, process, or service by trade name, trademark, manufacturer, or otherwise does not necessarily constitute or imply its endorsement, recommendation, or favoring by the U.S. Government or any agency thereof. The views and opinions of authors expressed herein do not necessarily state or reflect those of the U.S. Government or any agency thereof.

*Corresponding author.
gatu@psfc.mit.edu.

[1] S. Quaglioni, C. Romero-Redondo, and P. Navrátil, Phys. Rev. C **88**, 034320 (2013).
[2] C. Romero-Redondo, S. Quaglioni, P. Navrátil, and G. Hupin, Phys. Rev. Lett. **113**, 032503 (2014).
[3] C. Romero-Redondo, S. Quaglioni, P. Navrátil, and G. Hupin, Phys. Rev. Lett. **117**, 222501 (2016).
[4] S. Quaglioni *et al.*, Phys. Rev. C **97**, 034332 (2018).
[5] M. B. Chadwick *et al.*, Nucl. Data Sheets **107**, 2931 (2006).
[6] V. I. Serov, S. N. Abramovich, and L. A. Morkin, At. Energ. **42**, 66 (1977).
[7] A. M. Govorov, K.-Y. Li, G. M. Osetinskii, V. I. Salatskii, and I. V. Sizov, Sov. Phys. JETP **15**, 266 (1962).
[8] N. Jarmie and R. C. Allen, Phys. Rev. **111**, 1121 (1958).
[9] H. M. Agnew, W. T. Leland, H. V. Argo, R. W. Crews, A. H. Hemmendinger, W. E. Scott, and R. F. Taschek, Phys. Rev. **84**, 862 (1951).
[10] D. T. Casey *et al.*, Nat. Phys. **13**, 1227 (2017).
[11] C. Wong, J. D. Anderson, and J. W. McClure, Nucl. Phys. **71**, 106 (1965).
[12] S. Typel, G. Bluge, K. Langanke, and W. A. Fowler, Z. Phys. A **339**, 249 (1991).
[13] C. Angulo and P. Descouvemont, Nucl. Phys. **A639**, 733 (1998).
[14] D. T. Casey, J. A. Frenje, M. Gatu Johnson, M. J.-E. Manuel, N. Sinenian, A. B. Zylstra, F. H. Seguin, C. K. Li, R. D. Petrasso, V. Y. Glebov, P. B. Radha, D. D. Meyerhofer, T. C. Sangster, D. P. McNabb, P. A. Amendt, R. N. Boyd, S. P. Hatchett, S. Quaglioni, J. R. Rygg, I. J. Thompson *et al.*, Phys. Rev. Lett. **109**, 025003 (2012).
[15] K. W. Allen, E. Almqvist, J. T. Dewan, T. P. Pepper, and J. H. Sanders, Phys. Rev. **82**, 262 (1951).
[16] R. Larose-Potissou and H. Jeremie, Nucl. Phys. **A218**, 559 (1974).
[17] T. Matsuzaki *et al.*, Phys. Lett. B **557**, 176 (2003).
[18] D. B. Sayre, C. R. Brune, J. A. Caggiano, V. Y. Glebov, R. Hatarik, A. D. Bacher, D. L. Bleuel, D. T. Casey, C. J. Cerjan, M. J. Eckart, R. J. Fortner, J. A. Frenje, S. Friedrich, M. Gatu-Johnson, G. P. Grim, C. Hagmann, J. P. Knauer, J. L. Kline, D. P. McNabb, J. M. McNaney *et al.*, Phys. Rev. Lett. **111**, 052501 (2013).
[19] T. R. Boehly *et al.*, Opt. Commun. **133**, 495 (1997).
[20] E. G. Adelberger *et al.*, Rev. Mod. Phys. **83**, 195 (2011).
[21] A. Krauss, H. W. Becker, H. P. Trautvetter, and C. Rolfs, Nucl. Phys. **A467**, 273 (1987).
[22] R. Bonetti *et al.*, Phys. Rev. Lett. **82**, 5205 (1999).
[23] M. Junker *et al.*, Phys. Rev. C **57**, 2700 (1998).
[24] N. Kudomi, M. Komori, K. Takahisa, S. Yoshida, K. Kume, H. Ohsumi, and T. Itahashi, Phys. Rev. C **69**, 015802 (2004).

[25] C. R. Brune, J. A. Caggiano, D. B. Sayre, A. D. Bacher, G. M. Hale, and M. W. Paris, Phys. Rev. C **92**, 014003 (2015).
[26] L. Ballabio, J. Källne, and G. Gorini, Nucl. Fusion **38**, 1723 (1998).
[27] M. Gatu Johnson *et al.*, Phys. Plasmas **24**, 041407 (2017).
[28] C. Iliadis, *Nuclear Physics of Stars: Second, Revised and Enlarged Edition* (Wiley-VCH, Berlin, 2015).
[29] J. T. Larsen and S. M. Lane, J. Quant. Spectrosc. Radiat. Transfer **51**, 179 (1994).
[30] C. Forrest, R. Bahukutumbi, V. Glebov, V. Goncharov, J. Knauer, A. Pruyne, M. Romanofsky, T. Sangster, M. Shoup III, C. Stoeckl, D. Casey, M. Gatu Johnson, and S. Gardner, Rev. Sci. Instrum. **83**, 10D919 (2012).
[31] C. J. Forrest, V. Yu. Glebov, V. N. Goncharov, J. P. Knauer, P. B. Radha, S. P. Regan, M. H. Romanofsky, T. C. Sangster, M. J. Shoup III, and C. Stoeckl, Rev. Sci. Instrum. **87**, 11D814 (2016).
[32] In ICF, the timescale for a burn is short enough where the implosion time can be used as the start signal, and only a single detector is required for the NTOF measurement (the burn duration for these implosions is ∼100 ps). Neglecting the impulse response of the detector, $E = 0.5m \times d^2/t^2$, where m is the neutron mass, d the detector distance, and t the flight time.
[33] Photek Ltd., St. Leonards-on-Sea, East Sussex TN38 9NS, United Kingdom.
[34] V. V. Verbinski, W. R. Burrus, T. A. Love, W. Zobel, N. W. Hill, and R. Textor, Nucl. Instrum. Methods **65**, 8 (1968).
[35] R. L. Craun and D. L. Smith, Nucl. Instrum. Methods **80**, 239 (1970).
[36] Given the challenges in assigning statistical error bars, the χ^2_{red} value should not be considered as a strict statistical metric for quality of fit. Inspection of Fig. 3 demonstrates the quality of the fit with $\chi^2_{\mathrm{red}} = 2.0$.
[37] See Supplemental material at http://link.aps.org/supplemental/10.1103/PhysRevLett.121.042501 for feeding factor results for each fit performed.
[38] D. R. Thompson and Y. C. Tang, Nucl. Phys. **A106**, 591 (1968).
[39] K. Arai, K. Kato, and S. Aoyama, Phys. Rev. C **74**, 034305 (2006).